

## Supporting Information

# Theoretical Insights into Promotion Effect of Alkali Metal Cations on Electroreduction Mechanism of CO<sub>2</sub> into C<sub>1</sub> Products at Cu(111)/H<sub>2</sub>O Interface

Lihui Ou<sup>1\*</sup>, Hai Yang<sup>2\*</sup>, Junling Jin<sup>1</sup>, Yuandao Chen<sup>1</sup>

### 1. Computational Details

#### 1.1 Surface and Solvation Model

The closed-packed Cu(111) single-crystal surface is generally chosen as representative crystal plane for both experimental and theoretical studies due to its high selectivity to CO<sub>2</sub> electroreduction into C<sub>1</sub> products. Considering complexity of real CO<sub>2</sub> electroreduction systems, the aqueous-phase environment is included. Our present solvation model is on the basis of the previous experimental and theoretical studies on structure and orientation of H<sub>2</sub>O molecules,<sup>1-3</sup> where 12 explicit H<sub>2</sub>O molecules with two relaxed bilayer structures were employed to simulate solvation effect in order to better model interactions between solvent and adsorbates and decrease size of the simulated systems as much as possible. Considering the coverage is 2/3 of H<sub>2</sub>O monolayer, therefore, a (3x3) Cu(111) slab model with nine metal atoms per layer and theoretical equilibrium lattice constant of 3.66 Å by using four metal layers was created. Alkali metals Na and Cs with different atomic size are incorporated into Cu(111)/H<sub>2</sub>O interface model in this paper. Alkali metal cations have been hypothesized to adsorb to the electrode surface or interact with surface-adsorbed species non-covalently.<sup>4, 5</sup> However, surface X-ray scattering data have suggested alkali metal cations to be solvated and not adsorbed at the electrode surface.<sup>6</sup> In this paper, alkali metals Na and Cs are initially adsorbed on Cu(111) surface. However, alkali metals are spontaneously solvated and not adsorbed on Cu(111) after geometry

---

<sup>1</sup>Hunan Province Cooperative Innovation Center for the Construction & Development of Dongting Lake Ecologic Economic Zone, Hunan Provincial Key Laboratory of Water Treatment Functional Materials, Hunan Province Engineering Research Center of Electroplating Wastewater Reuse Technology, College of Chemistry and Materials Engineering, Hunan University of Arts and Science, Changde, 415000, China. E-mail: [lihuiou@huas.edu.cn](mailto:lihuiou@huas.edu.cn)

<sup>2</sup>Hunan Provincial Key Laboratory of Environmental Catalysis & Waste Recycling, Hunan Institute of Engineering, Xiangtan, 411104, PR China. [yanghai1001@163.com](mailto:yanghai1001@163.com)

Electronic supplementary information (ESI) available.

relaxation and optimization, confirming experimental observations, as can be seen in Fig. S1.

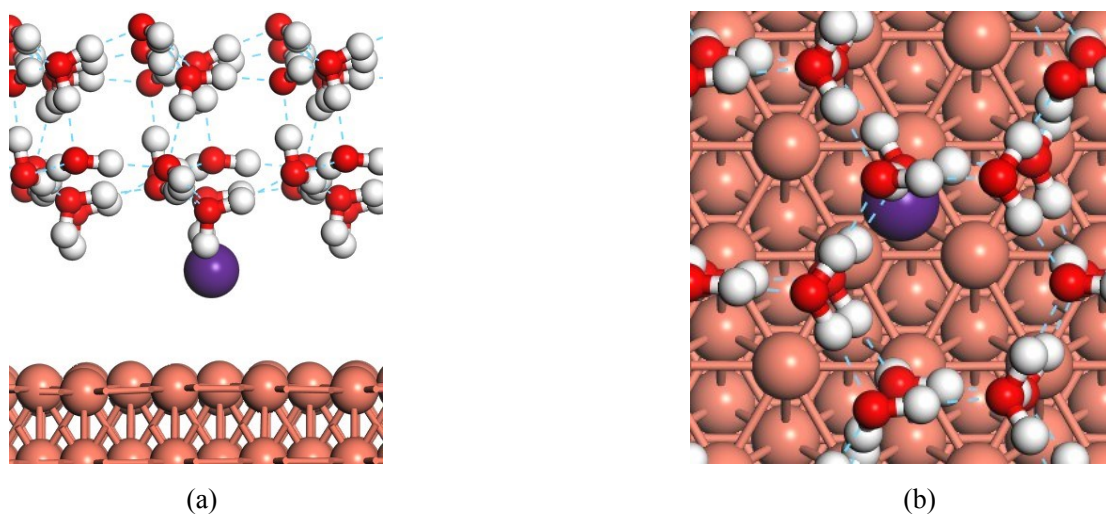


**Fig. S1.** The Solvation Model Containing Alkali Metal Cations on Cu(111): (a) Side View; (b) Top View.

## 1.2 CO Coverage-Dependent Equilibrium Potential

As elaborated in our recent study,<sup>7</sup> the differential adsorption energy of CO,  $\Delta E(\theta)$  exhibits reasonable linear dependence on  $\theta_{\text{CO}}$  on Cu(111). Linearly fitting  $\Delta E(\theta) \sim \theta_{\text{CO}}$  data to straight line enables us calculate  $\Delta E(\theta)$  at any  $\theta_{\text{CO}}$ . Thus, the linear relationships between CO coverage ( $\theta_{\text{CO}}$ ) and the calculated equilibrium potentials ( $U$ ) can be obtained on Cu(111). It can be observed that more CO coverage will lead to more negative equilibrium potential for CO<sub>2</sub> electroreduction, suggesting that overpotential may mainly originate from the adsorbed CO on Cu electrodes. The calculated thermodynamical equilibrium potential is *ca.* 0.27 V (*vs.* RHE) when  $\theta_{\text{CO}}$  is closely zero, which is comparable with thermodynamical equilibrium potential of 0.17 V (*vs.* RHE) for CO<sub>2</sub> electroreduction from literature and confirm the reasonability of the present theoretical model to some degree.<sup>8</sup> Our recent study focused on CO adsorption with low coverage of 1/9 ML on clean Cu(111) and calculated equilibrium potential is *ca.* 0.14 V (*vs.* RHE),<sup>7</sup> corresponding to the condition of low overpotential compared with thermodynamical equilibrium potential when  $\theta_{\text{CO}}$  is closely zero (*ca.* 0.13 V). In this paper, alkali metals Na with smaller atomic size and Cs with relatively larger atomic size are integrated into our recent proposed CO coverage-dependent Cu(111)/H<sub>2</sub>O electrochemical interface model, which are used to study influences of alkali metal cations on CO<sub>2</sub> electroreduction mechanisms in aqueous electrolyte.

## 1.3 Computational Parameters

All calculations were performed in the framework of DFT using the generalized gradient approximation

of Perdew–Burke–Ernzerhof exchange correlation functional.<sup>9</sup> Ultrasoft pseudopotentials were employed to describe the nuclei and core electrons and a plane-wave basis set was used to self-consistently solve the Kohn-Sam equations.<sup>10</sup> A kinetic energy cutoff of 30 Ry and a charge-density cutoff of 300 Ry were used to make basis set finite. The smearing technique of Methfessel-Paxton was employed to treat the Fermi surface with a smearing parameter of 0.02 Ry.<sup>11</sup> All DFT calculations were carried out by the PWSCF codes included in Quantum ESPRESSO distribution.<sup>12</sup> A  $(3 \times 3 \times 1)$  uniformly shifted k-mesh for  $(3 \times 3)$  supercell were used to implement Brillouin-zone integrations with the special-point technique. A vacuum layer of 16Å was placed above the top layer of slab, which is sufficiently large to ensure that the interactions are negligible between repeated slabs. The Cu atoms in the bottom two layers are fixed at the theoretical bulk positions, whereas the top two layers and adsorbates involving solvent are allowed to relax. Structural optimization was performed until the Cartesian force components acting on each atom were brought below  $10^{-3}$  Ry/Bohr and the total energy was converged to within  $10^{-5}$  Ry. The saddle points and minimum energy paths (MEPs) were located by using the climbing image nudged elastic band (CI-NEB) method.<sup>13, 14</sup> Zero point energy (ZPE) corrections were applied into calculations of the activation and reaction energies from MEP analysis, in which density functional perturbation theory was used to study the vibrational properties.<sup>15</sup> The ZPEs were calculated using the PHONONS code that contained in the Quantum ESPRESSO distribution.<sup>12</sup>

## 2. Minimum Energy Pathway (MEP) Analysis

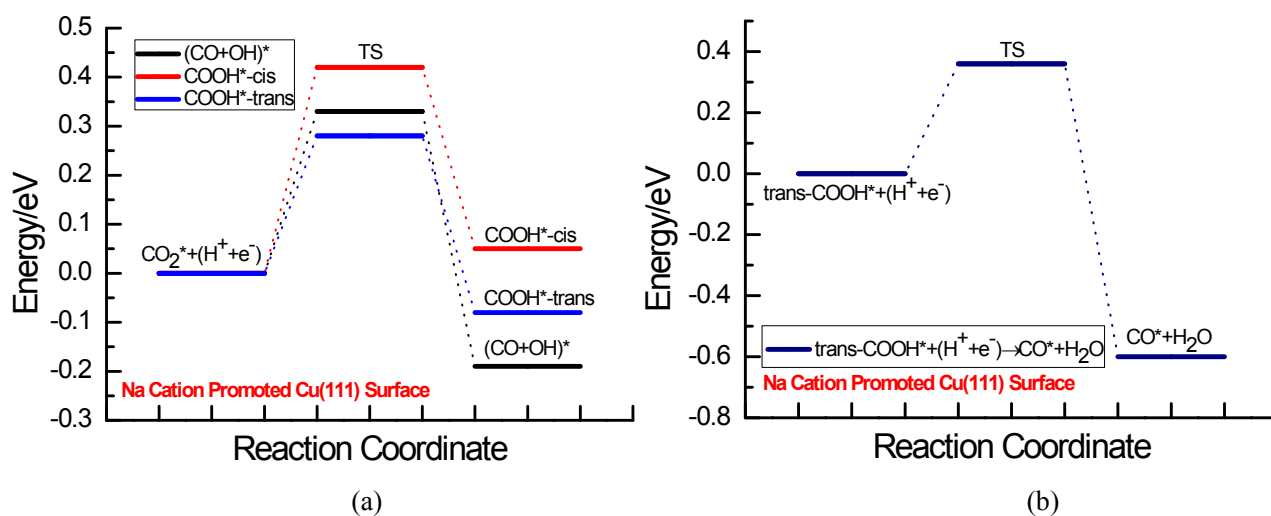


**Fig. S2.** The MEP analysis of (a) the first elementary step of  $\text{CO}_2$  electroreduction and (b) subsequent *trans*-COOH electroreduction into CO and  $\text{H}_2\text{O}$  at Na cation promoted Cu(111)/ $\text{H}_2\text{O}$  interface (an asterisk \* indicates

adsorption to the Cu surface)

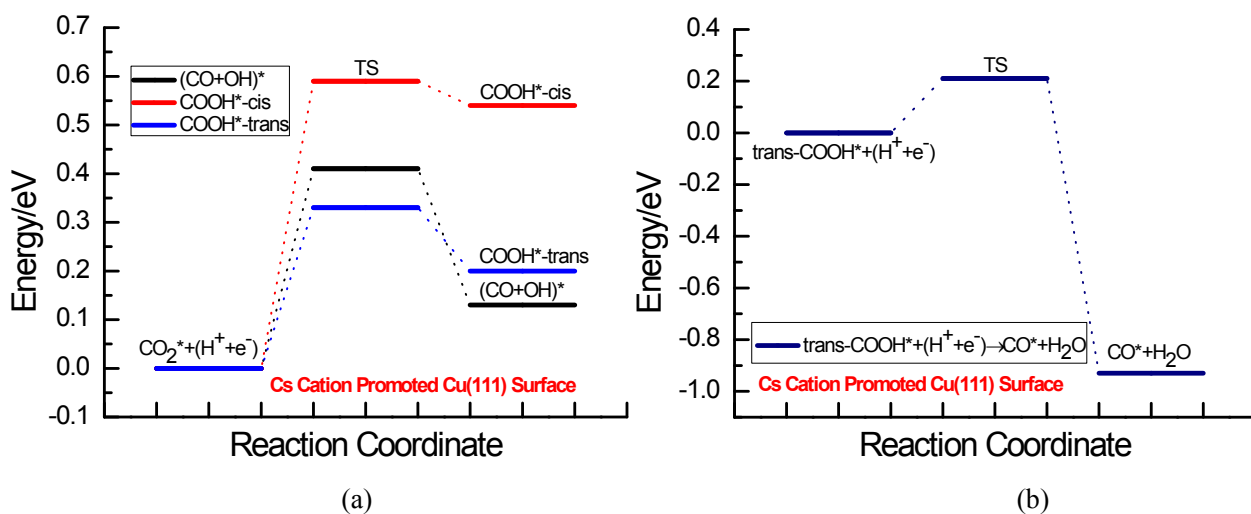


**Fig. S3.** The MEP analysis of (a) the first elementary step of CO<sub>2</sub> electroreduction and (b) subsequent *trans*-COOH electroreduction into CO and H<sub>2</sub>O at Cs cation promoted Cu(111)/H<sub>2</sub>O interface (an asterisk \* indicates adsorption to the Cu surface)

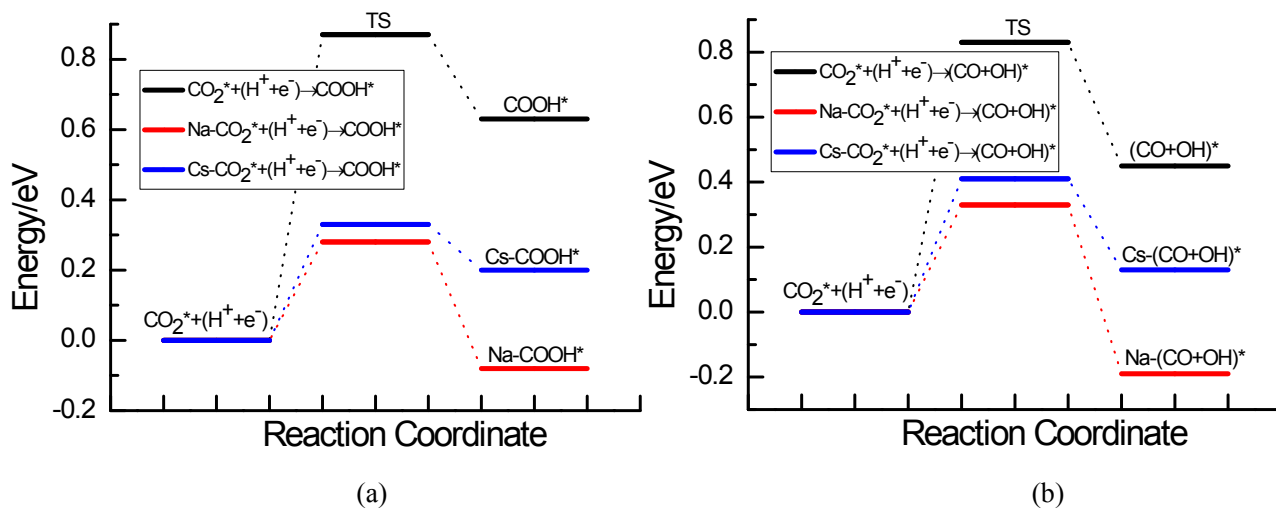


**Fig. S4.** The MEP analysis of (a) CO<sub>2</sub> electroreduction into COOH species; (b) CO<sub>2</sub> electroreduction into CO intermediate at clean, Na and Cs cations promoted Cu(111)/H<sub>2</sub>O interface (an asterisk \* indicates adsorption to the Cu surface)

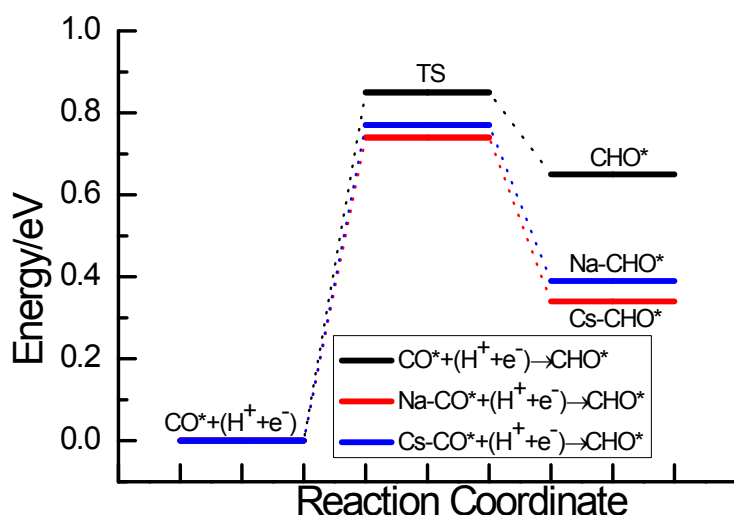


**Fig. S5.** The MEP analysis of CO electroreduction into CHO species intermediate at clean, Na and Cs cations promoted Cu(111)/H<sub>2</sub>O interface (an asterisk \* indicates adsorption to the Cu surface)

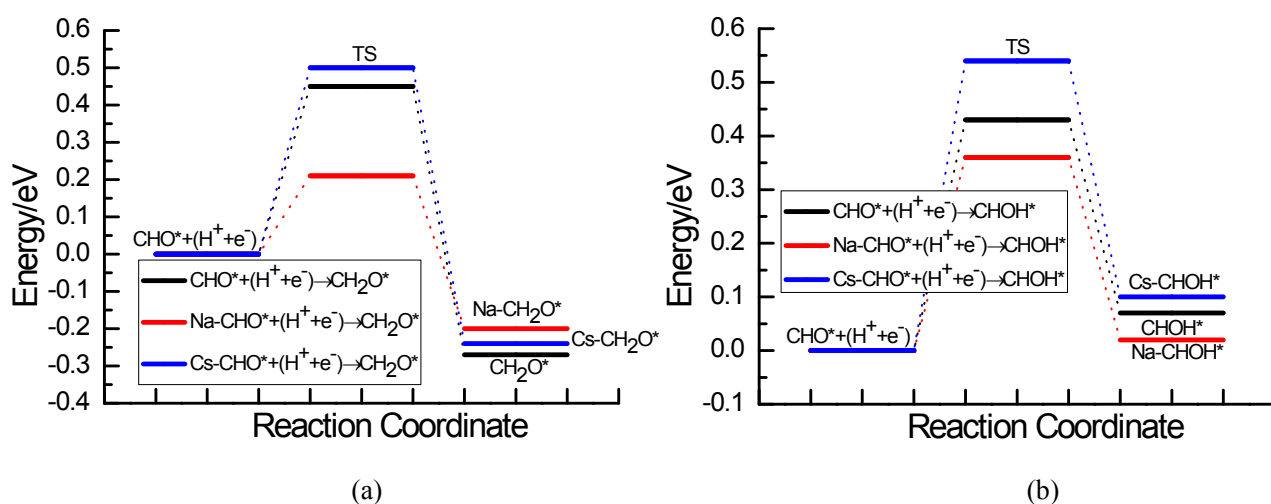


**Fig. S6.** The MEP analysis of (a) CHO electroreduction into CH<sub>2</sub>O species; (b) CHO electroreduction into CHOH species at clean, Na and Cs cations promoted Cu(111)/H<sub>2</sub>O interface (an asterisk \* indicates adsorption to the Cu surface)

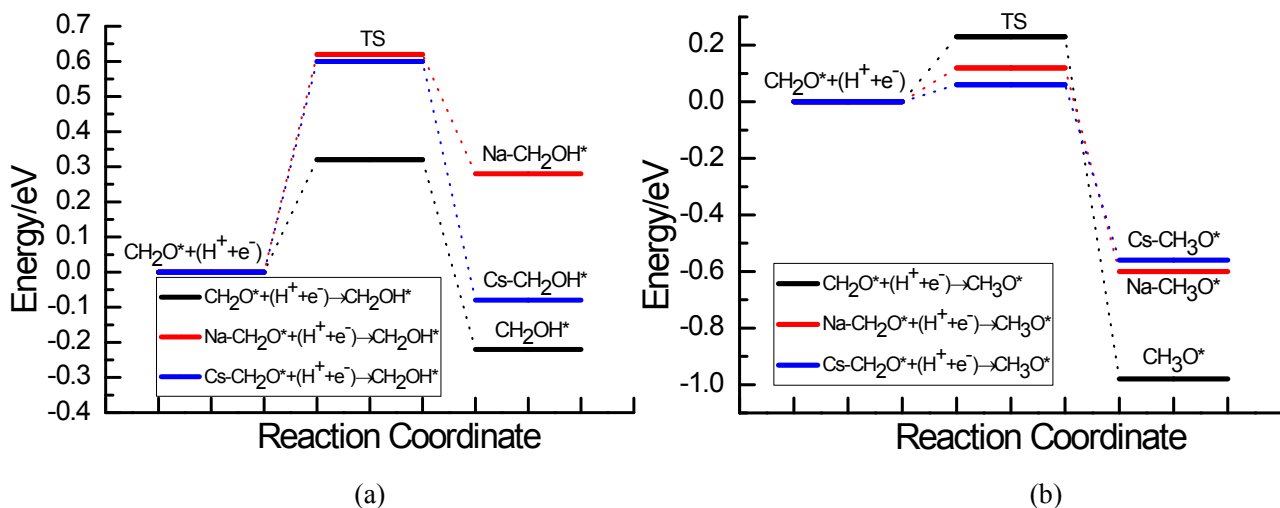


**Fig. S7.** The MEP analysis of (a)  $\text{CH}_2\text{O}$  electroreduction into  $\text{CH}_2\text{OH}$  species; (b)  $\text{CH}_2\text{O}$  electroreduction into  $\text{CH}_3\text{O}$  species at clean, Na and Cs cations promoted  $\text{Cu}(111)/\text{H}_2\text{O}$  interface (an asterisk \* indicates adsorption to the Cu surface)

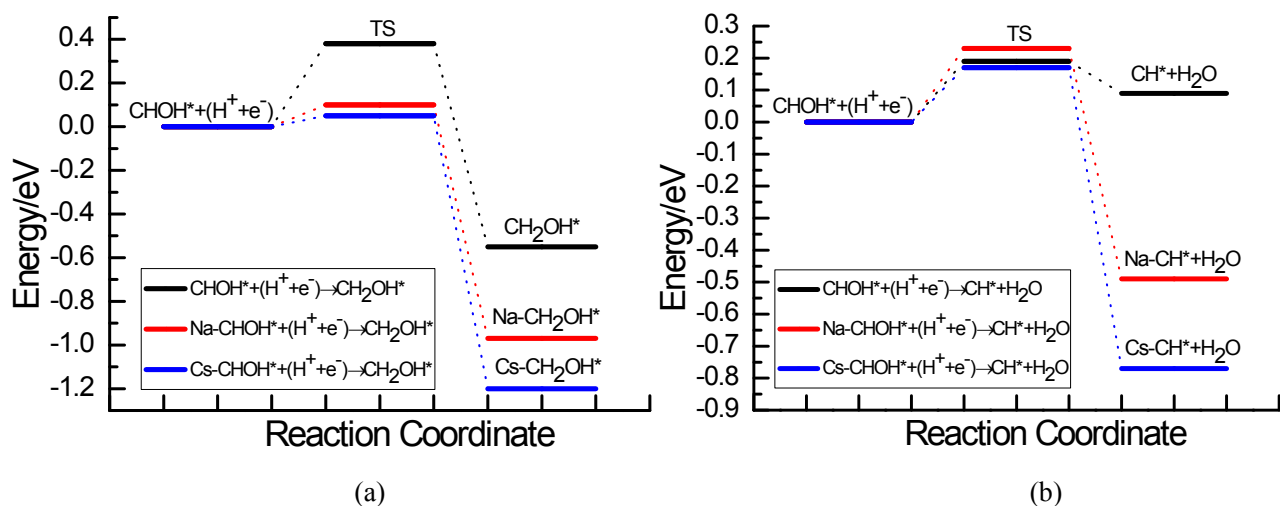


**Fig. S8.** The MEP analysis of (a)  $\text{CHO}$  electroreduction into  $\text{CH}_2\text{OH}$  species; (b)  $\text{CHO}$  electroreduction into  $\text{CH}$  species along with  $\text{H}_2\text{O}$  formation at clean, Na and Cs cations promoted  $\text{Cu}(111)/\text{H}_2\text{O}$  interface (an asterisk \* indicates adsorption to the Cu surface)

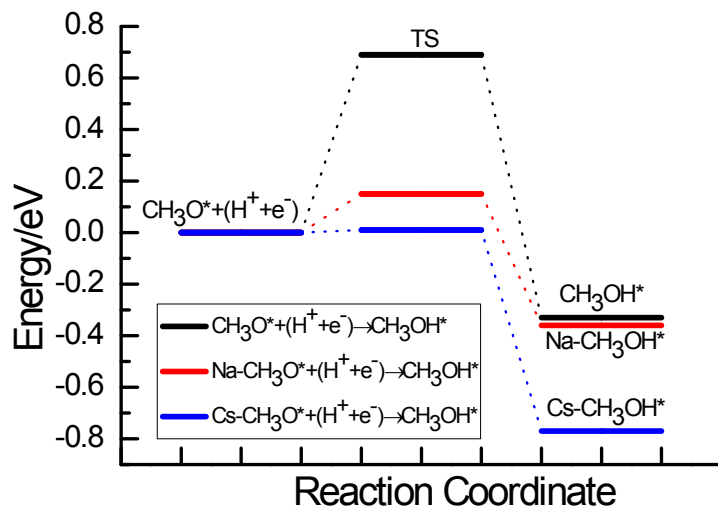


**Fig. S9.** The MEP analysis of  $\text{CH}_3\text{O}$  electroreduction into  $\text{CH}_3\text{OH}$  product at clean, Na and Cs cations promoted Cu(111)/ $\text{H}_2\text{O}$  interface (an asterisk \* indicates adsorption to the Cu surface)

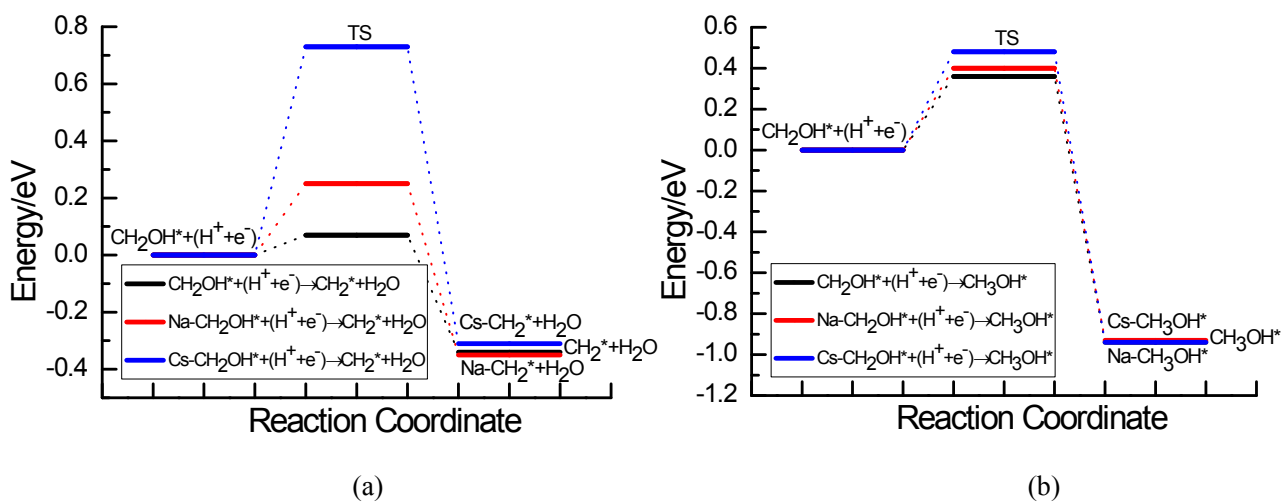


**Fig. S10.** The MEP analysis of (a)  $\text{CH}_2\text{OH}$  electroreduction into  $\text{CH}_2$  species along with  $\text{H}_2\text{O}$  formation; (b)  $\text{CH}_2\text{OH}$  electroreduction into  $\text{CH}_3\text{OH}$  product at clean, Na and Cs cations promoted Cu(111)/ $\text{H}_2\text{O}$  interface (an asterisk \* indicates adsorption to the Cu surface)

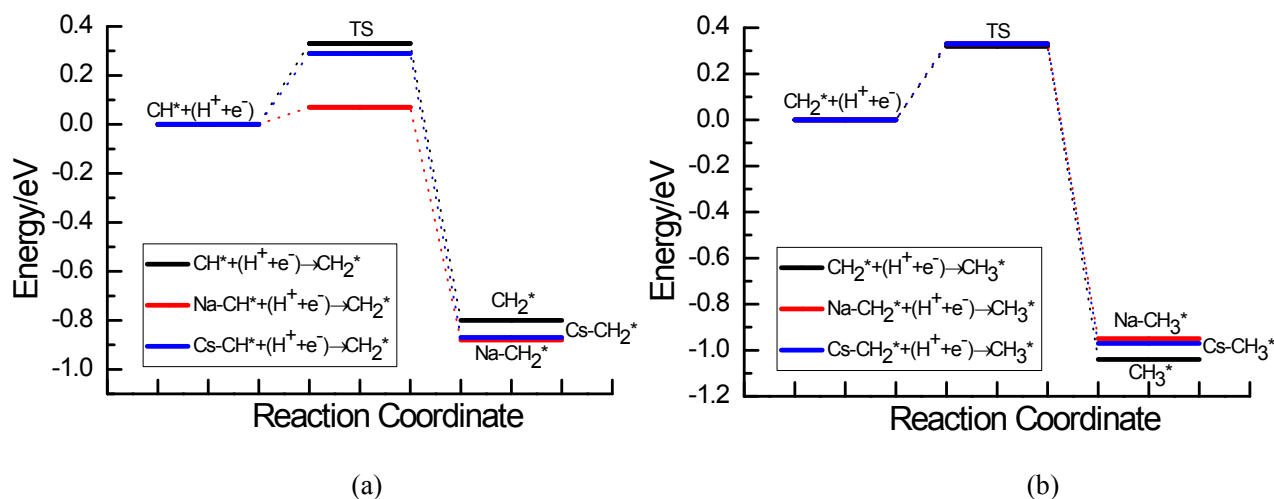


**Fig. S11.** The MEP analysis of (a) CH electroreduction into CH<sub>2</sub> species; (b) CH<sub>2</sub> electroreduction into CH<sub>3</sub> species at clean, Na and Cs cations promoted Cu(111)/H<sub>2</sub>O interface (an asterisk \* indicates adsorption to the Cu surface)

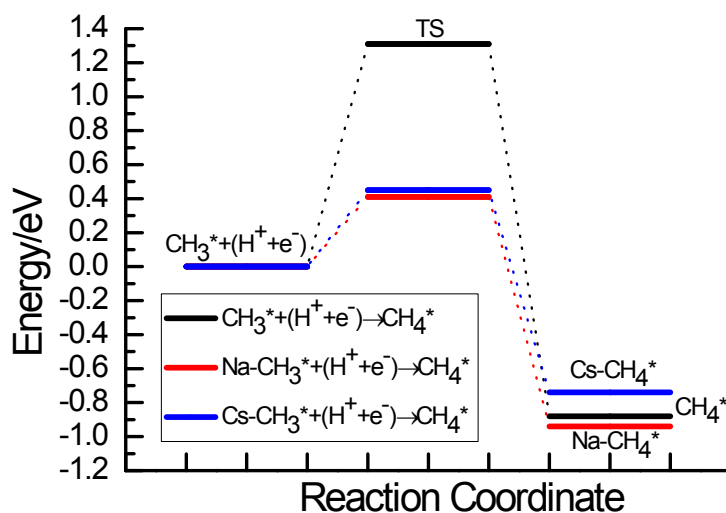


**Fig. S12.** The MEP analysis of CH<sub>3</sub> electroreduction into CH<sub>4</sub> product at clean, Na and Cs cations promoted Cu(111)/H<sub>2</sub>O interface (an asterisk \* indicates adsorption to the Cu surface)

## References

- 1 E. Skúlason, V. Tripkovic, M. E. Björketun, S. Gudmundsdóttir, G. Karlberg, J. Rossmeisl, T. Bligaard, H. Jónsson, J. K. Nørskov, Modeling the Electrochemical Hydrogen Oxidation and Evolution Reactions on the Basis of Density Functional Theory Calculations, *J. Phys. Chem. C*, 2010, **114**, 18182-18197.
- 2 M. A. Henderson, Interaction of Water with Solid surfaces: Fundamental Aspects Revisited, *Surf. Sci. Rep.*, 2002, **46**, 1-308.



- 3 H. Ogasawara, B. Brena, D. Nordlund, M. Nyberg, A. Pelmeshnikov, L. G. M. Pettersson and A. Nilsson, Structure and Bonding of Water on Pt(111), *Phys. Rev. Lett.*, 2002, **89**, 276102.
- 4 D. Strmcnik, K. Kodama, D. van der Vliet, J. Greeley, V. R. Stamenkovic and N. M. Marković, The Role of Non-Covalent Interactions in Electrocatalytic Fuel-Cell Reactions on Platinum, *Nat. Chem.*, 2009, **1**, 466-472.
- 5 C. Stoffelsma, P. Rodriguez, G. Garcia, N. Garcia-Araez, D. Strmcnik, N. M. Marković and M. T. M. Koper, Promotion of the Oxidation of Carbon Monoxide at Stepped Platinum Single-Crystal Electrodes in Alkaline Media by Lithium and Beryllium Cations, *J. Am. Chem. Soc.*, 2010, **132**, 16127-16133.
- 6 D. Strmcnik, D. van der Vliet, K. C. Chang, V. Komanicky, K. Kodama, H. You, V. R. Stamenkovic and N. M. Marković, Effects of Li<sup>+</sup>, K<sup>+</sup>, and Ba<sup>2+</sup> Cations on the ORR at Model and High Surface Area Pt and Au Surfaces in Alkaline Solutions, *J. Phys. Chem. Lett.*, 2011, **2**, 2733-2736.
- 7 L. H. Ou, J. X. Chen, Y. D. Chen and J. L. Jin, Mechanistic study on Cu-catalyzed CO<sub>2</sub> Electroreduction into CH<sub>4</sub> at Simulated Low Overpotentials Based on an Improved Electrochemical Model, *Phys. Chem. Chem. Phys.*, 2019, **21**, 15531-15540.
- 8 A. A. Peterson, F. Abild-Pederson, F. Studt, J. Rossmeisl and J. K. Nørskov, How Copper Catalyzes the Electroreduction of Carbon Dioxide into Hydrocarbon Fuels, *Energy Environ. Sci.*, 2010, **3**, 1311-1315.
- 9 J. P. Perdew, K. Burke and M. Ernzerhof, Generalized Gradient Approximation Made Simple, *Phys. Rev. Lett.*, 1996, **77**, 3865-3868.
- 10 D. Vanderbilt, Soft Self-Consistent Pseudopotentials in a Generalized Eigenvalue Formalism, *Phys. Rev. B*, 1990, **41**, 7892-7895.
- 11 M. Methfessel and A. T. Paxton, High-Precision Sampling for Brillouin-Zone Integration in Metals, *Phys. Rev. B*, 1989, **40**, 3616-3621.
- 12 S. Baroni, A. Dal Corso, S. de Gironcoli and P. Giannozzi, PWSCF and PHONON: Plane-Wave Pseudopotential Codes. <http://www.quantum-espresso.org/>, 2001.
- 13 G. Henkelman and H. Jonsson, Improved Tangent Estimate in the Nudged Elastic Band Method for Finding Minimum Energy Paths and Saddle Points, *J. Chem. Phys.*, 2000, **113**, 9978-9985.
- 14 G. Henkelman, B. P. Uberuaga and H. Jonsson, A Climbing Image Nudged Elastic Band Method for Finding Saddle Points and Minimum Energy Paths, *J. Chem. Phys.*, 2000, **113**, 9901-9904.
- 15 S. Baroni, S. Gironcoli, A. Corso and P. Giannozzi, Phonons and Related Properties of Extended Systems from Density Functional Perturbation Theory, *Rev. Mod. Phys.*, 2001, **73**, 515-562.